

LETTER TO THE EDITOR

A non-equilibrium ortho-to-para ratio of water in the Orion PDR[★]

Y. Choi^{1,2}, F. F. S. van der Tak^{2,1}, E. A. Bergin³, R. Plume⁴

¹ Kapteyn Astronomical Institute, University of Groningen, P.O. Box 800, 9700 AV, Groningen, The Netherlands
e-mail: y.choi@astro.rug.nl

² SRON Netherlands Institute for Space Research, P.O. Box 800, 9700 AV, Groningen, The Netherlands

³ Department of Astronomy, University of Michigan, 500 Church Street, Ann Arbor, MI 48109, USA

⁴ Department of Physics and Astronomy, University of Calgary, 2500 University Drive NW, Calgary, AB T2N 1N4, Canada

July 27, 2018

ABSTRACT

Context. The ortho-to-para ratio (OPR) of H₂O is thought to be sensitive to the temperature of water formation. The OPR of H₂O is thus useful to study the formation mechanism of water.

Aims. We investigate the OPR of water in the Orion PDR (Photon-dominated region), at the Orion Bar and Orion S positions, using data from *Herschel*/HIFI.

Methods. We detect the ground-state lines of ortho- and para-H₂¹⁸O in the Orion Bar and Orion S and we estimate the column densities using LTE and non-LTE methods.

Results. Based on our calculations, the ortho-to-para ratio (OPR) in the Orion Bar is 0.1 – 0.5, which is unexpectedly low given the gas temperature of ~ 85 K, and also lower than the values measured for other interstellar clouds and protoplanetary disks. Toward Orion S, our OPR estimate is below 2.

Conclusions. This low OPR at 2 positions in the Orion PDR is inconsistent with gas phase formation and with thermal evaporation from dust grains, but it may be explained by photodesorption.

Key words. ISM: molecules – ISM: individual objects: Orion Bar, Orion S

1. Introduction

Water is an important reservoir of interstellar oxygen and therefore a key ingredient in the chemistry of oxygen-bearing molecules. In the interstellar medium, water can be formed by three different mechanisms. In cold molecular clouds, water may be formed in the gas phase by ion-molecule chemistry, through dissociative recombination of H₃O⁺. In cold and dense cores, on the surfaces of cold dust grains, O and H atoms may combine to form water-rich ice mantles. These mantles will evaporate when the grains are heated to ~ 100 K by protostellar radiation or sputtered by outflow shocks. Third, in gas with temperatures above 300 K, reactions of O and OH with H₂ drive all gas-phase oxygen into water. Such high temperatures may occur very close to the star due to heating by protostellar radiation, or outflow shocks (see van Dishoeck et al. 2013, for a review).

The hydrogen atom carries a nuclear spin angular momentum and two species of molecular hydrogen exist (ortho-H₂ and para-H₂). Other molecules with two or more hydrogen atoms also exhibit this characteristic with two independent spin isomers (e.g., H₂O, NH₃, CH₄). Because of a difference in the energy of the rotational ground state (34 K for ortho-H₂O, 0 K for para-H₂O) the ratio of ortho to para water vapor is dependent on the gas temperature in thermal equilibrium. Above 40 K the OPR would be the ratio of the spin statistical weights of 3 and below this temperature there is an expectation that the formation of para-H₂O would be successively favored over ortho-H₂O

leading to a reduced OPR (Mumma et al. 1987). Since inelastic collisions do not change the OPR, this ratio may provide clues to the formation mechanism of water. The measured OPRs of H₂O is 2–3 in solar system comets (Mumma & Charnley 2011) and in Galactic interstellar clouds (Lis et al. 2013; Flagey et al. 2013), while an OPR of ~1 was measured for water vapor in the TW Hya disk (Hogerheijde et al. 2011).

In this paper we will present measurements of the rotational emission of both spin isomers of water vapor towards the Orion photon-dominated region. Photon-dominated regions (PDRs) are the surface regions of molecular clouds, where ultraviolet radiation with photon energies between 6 and 13.6 eV drives the thermal and chemical balance of the gas (Hollenbach & Tielens 1999). Shielding of the UV radiation by dust and gas creates a layered structure where a sequence of different chemical transitions is produced by the gradual attenuation of the UV field (Ossenkopf et al. 2007).

The Orion Molecular Cloud 1 (OMC-1), at a distance of ~ 420 pc (Menten et al. 2007), is one of the nearest massive star forming regions. Parts of the OMC-1 region are ionized by the Trapezium cluster creating an HII region. The Orion Bar PDR stands out as a ridge to the Southeast of the Trapezium cluster. Observations at infrared and submillimeter wavelengths indicate a geometry for the Bar where the PDR is wrapped around the HII region created by the Trapezium stars, and changes from a face-on to an edge-on view where the molecular emission peaks (Hogerheijde et al. 1995). The mean density of the Bar is about 10⁵ cm⁻³, and the gas temperature is 85 K in the interior, rising to ~ 150 K at the PDR surface (Larsson et al. 2003). The impinging radiation field is (1–4) × 10⁴ χ₀, where the Draine field

[★] *Herschel* is an ESA space observatory with science instruments provided by European-led Principal Investigator consortia and with important participation from NASA.

Table 1. Observed lines.

Source	Molecule	Transition	ν (GHz)	E_{up} (K)	T_{sys} (K)	t_{int} (min)	Beam ($''$)	η_{mb}	$\delta\nu$ (MHz)	rms (mK)
Orion Bar	o-H ₂ ¹⁸ O	1 ₁₀ – 1 ₀₁	547.676	60.5	63	88	38.7	0.75	0.48	2.67
	p-H ₂ ¹⁸ O	1 ₁₁ – 0 ₀₀	1101.698	53.4	350	56	19.2	0.74	1.1	102
Orion S	o-H ₂ ¹⁸ O	1 ₁₀ – 1 ₀₁	547.676	60.5	71	7.4	38.7	0.75	1.1	26
	p-H ₂ ¹⁸ O	1 ₁₁ – 0 ₀₀	1101.698	53.4	366	10	19.2	0.74	1.1	121

$\chi_0 = 2.7 \times 10^{-3} \text{ erg s}^{-1} \text{ cm}^{-2}$ (Draine 1978). The clumpiness of the PDR inferred by Hogerheijde et al. (1995) is confirmed by interferometric data (Lis & Schilke 2003), with densities of up to 1.5×10^6 to $6 \times 10^6 \text{ cm}^{-3}$. In contrast the densities of the interclump medium fall between a few 10^4 cm^{-3} (Young Owl et al. 2000) and $2 \times 10^5 \text{ cm}^{-3}$ (Simon et al. 1997).

Orion S is an active star-forming region, located 1' southwest of the Trapezium, as indicated by the number of outflows and Herbig-Haro flows (Zapata et al. 2006). The mass of Orion S is $\sim 100 M_{\odot}$ and the size of this region is similar to that of Orion BN/KL, but its bolometric luminosity of $10^4 L_{\odot}$ is an order of magnitude lower (Mezger et al. 1990), which may indicate that Orion S is less evolved (McMullin et al. 1993). The UV radiation field is estimated to be $\chi \sim 1.5 \times 10^5 \chi_0$ at the position of Orion S (Herrmann et al. 1997), about a factor of 10 higher than that in the Orion Bar. Due to the irradiation by the nearby Trapezium cluster, the part of the Orion S region facing the Trapezium cluster includes an ionization front and a face-on PDR.

This paper uses *Herschel*/HIFI observations of water lines in the Orion PDR, at the Orion Bar and Orion S positions. With its much higher spatial and spectral resolution and higher sensitivity than previous space missions, we investigate the ortho-to-para ratio of water, providing new information on the formation mechanism of water in these regions.

2. Observations

The CO⁺ peak in the Orion Bar was observed with the Heterodyne Instrument for the Far-Infrared (HIFI, de Graauw et al. 2010) onboard ESA's *Herschel* Space Observatory (Pilbratt et al. 2010), in all HIFI bands as part of the *Herschel* observations of EXtra-Ordinary Sources (HEXOS) guaranteed-time key program (Bergin et al. 2010). The coordinates of the observed position of the CO⁺ peak in the Orion Bar are $05^{\text{h}}35^{\text{m}}20^{\text{s}}.6$ and $-05^{\circ}25'14''$ (J2000).

In this paper we use the p-H₂¹⁸O 1₁₁ – 0₀₀ line from the HIFI band 4b spectral line survey. This observation was carried out in April 2011 in load chop mode with a redundancy of 4 and with a total integration time of 0.7 h. The Wide-Band Spectrometer (WBS) backend was used which covers 4 GHz bandwidth in four 1140 MHz subbands at 1.1 MHz resolution. In addition to the HIFI spectral scan, the o-H₂¹⁸O 1₁₀ – 1₀₁ line was observed in September 2010 as a deep integration with a total integration time of 1.5 h in frequency switch mode.

Orion S was observed with a complete HIFI spectral scan as part of the HEXOS program. The observations were pointed toward $05^{\text{h}}35^{\text{m}}13^{\text{s}}.4$ and $-05^{\circ}24'08''.1$ (J2000). We use data from HIFI bands 1a (o-H₂¹⁸O 1₁₀ – 1₀₁) and 4b (p-H₂¹⁸O 1₁₁ – 0₀₀). The scans were observed using dual beam switch (DBS) observing mode. The WBS backend with a 1.1 MHz resolution was used.

We performed calibration of the data, removal of standing waves and spurs and sideband deconvolution using the *Herschel*

Interactive Processing Environment (HIPE, Ott 2010) version 10.0. Further analysis was done by the CLASS¹ package.

The frequencies, energy of the upper levels, system temperatures, integration times, and rms noise level at a given spectral resolution for each of the lines are provided in Table 1 along with the beam sizes and main beam efficiencies from Roelfsema et al. (2012).

3. Results

The HIFI spectra of the Orion Bar show pure single-peaked emission profiles in the ground-state lines of para- and ortho-H₂¹⁸O (Fig. A.1). In contrast, in Orion S, the ground-state line of ortho-H₂¹⁸O appears in emission but the ground-state line of para-H₂¹⁸O is detected in absorption (Fig. A.2). This effect may be due to the stronger continuum in Orion S than in the Orion Bar, which increases towards higher frequencies assuming the dust and gas are well mixed (continuum level ~ 4.6 K at 1101.7 GHz in Orion S compared to 0.3 K for the Bar). In addition, LVG models by Cernicharo et al. (2006) predict that ortho- and para-H₂O lines appear in absorption or emission depending on the adopted conditions.

We extract line parameters from the observed profiles by fitting Gaussians. The o-H₂¹⁸O 1₁₀ – 1₀₁ in Orion S has a hint of a self-reversal, but this is unfortunately at the level of noise in the data and the parameters of this line were determined by fitting one Gaussian; Table 2 gives the results for all lines. The components in the Orion Bar show similar line profiles, $\Delta V \sim 1.8 - 1.9 \text{ km s}^{-1}$ and $V_{\text{LSR}} \sim 10 \text{ km s}^{-1}$, suggesting that these two lines originate in the same gas. These parameters are also similar to those of CO, H₂CO and other dense gas tracers (Leurini et al. 2006). On the other hand, the line profiles in Orion S have a width of 4.6 – 5.5, which is broader than in the Orion Bar, and a velocity of $\sim 7.0 - 7.4 \text{ km s}^{-1}$. This velocity shift is commensurate with the known N-S velocity gradient seen along the Orion Molecular Ridge (Ungerechts et al. 1997). The observed line widths and LSR velocities are similar to those of CO isotopologues (Peng et al. 2012).

4. Analysis

4.1. Orion Bar

We estimate column densities assuming LTE and also explored models where the populations are not in LTE. For the LTE calculations, we have some additional supporting evidence based on other observations of both sources obtained as part of the HEXOS program. (1) The ground state lines of H₂¹⁷O are not detected (rms ~ 0.04 K at the o-H₂¹⁷O 1₁₀ – 1₀₁ line and rms ~ 0.2 K at the p-H₂¹⁷O 1₁₁ – 0₀₀ line) which limits the optical depth of the H₂¹⁸O lines to be below 0.7. In the following we assume that the emission is optically thin. (2) The water emission is not arising from very warm (> 100 K) and dense gas ($>$

¹ <http://www.iram.fr/IRAMFR/GILDAS/>

Table 2. Line parameters obtained from Gaussian fits.

Source	Molecule	Transition	$\int T_{\text{MB}} dV$ (K km s ⁻¹)	V_{LSR} (km s ⁻¹)	ΔV (km s ⁻¹)	T_{MB} (K)
Orion Bar	o-H ₂ ¹⁸ O	1 ₁₀ – 1 ₀₁	0.23 (0.01)	10.22 (0.01)	1.93 (0.03)	0.11
	p-H ₂ ¹⁸ O	1 ₁₁ – 0 ₀₀	0.56 (0.12)	9.91 (0.19)	1.84 (0.48)	0.29
Orion S	o-H ₂ ¹⁸ O	1 ₁₀ – 1 ₀₁	1.17 (0.06)	7.45 (0.13)	4.66 (0.27)	0.23
	p-H ₂ ¹⁸ O	1 ₁₁ – 0 ₀₀	3.48 (0.27)	7.05 (0.18)	5.53 (0.64)	-0.59 ^a

Notes. ^(a) Absorption line detected in Orion S

10⁸ cm⁻³) towards either the Orion Bar or Orion S as we do not detect emission arising from excited states (p-H₂¹⁸O 2₀₂ – 1₁₁, o-H₂¹⁸O 2₁₂ – 1₀₁, rms ~ 0.2 – 0.7 K), which implies a limit on the excitation temperature of less than 100 K. (3) The difference in beam size between the ortho-H₂¹⁸O 547 GHz line and para-H₂¹⁸O 1101 GHz line observations could lead us to underestimate the OPR by factors up to 4. However this is unlikely as water emission in the Orion ridge extends over several arcminutes (Melnick et al. 2011). Furthermore, the detected lines are likely to come from the same gas considering the velocities and line widths (see Table 2).

We therefore derive the column densities of ortho- and para-H₂¹⁸O in the Orion Bar for different excitation temperatures ($T_{\text{ex}} = 50 - 100$ K) and find values of $\sim 3.0 \times 10^{10}$ cm⁻² for the ortho-H₂¹⁸O line and $\sim 1.0 \times 10^{11}$ cm⁻² for the para-H₂¹⁸O line. The derived column densities are not strongly sensitive to the assumed excitation temperature. With the above assumptions, and in LTE, we derive an OPR of ~ 0.3 .

The ground state emission lines of ortho and para-water are not identical in their excitation characteristics. Moreover both lines have high critical densities and we therefore explore non-LTE models of H₂O using the RADEX code (van der Tak et al. 2007) and state-of-the-art quantum mechanical collision rates of para- and ortho-H₂O with para- and ortho-H₂ (Daniel et al. 2011) as provided at the LAMDA database (Schöier et al. 2005), assuming thermal values for the o/p ratio of H₂. For this exploration we generate a grid of models with values of $T_{\text{kin}} = 20, 60, \text{ and } 100$ K, values of $n(\text{H}_2) = 10^4, 10^6, \text{ and } 10^8$ cm⁻³, and fix the background radiation temperature at 2.73 K for the Orion Bar. Within the range of assumed densities and temperatures we find that the analysis remains consistent with a low OPR with values ranging from 0.1 to 0.5 (see Table B.1). For the case where H₂O emission is arising from the warm surface of the PDR, (e.g. Hollenbach et al. 2009), we perform an additional solution with $T_{\text{gas}} = 200$ K. For the density we use the detailed model of Nagy et al. (2013) which has a density of 10⁵ cm⁻³ at 200 K; with this assumption the derived ortho-to-para ratio is 0.14.

As an alternative background radiation field, we adopt a modified blackbody distribution with a dust temperature of $T_{\text{d}} = 49$ K and a dust emissivity index of $\beta = 1.6$ for the interior of the Orion Bar (Arab et al. 2012), so that the absolute dust opacity of $\tau_{\text{d}} = 0.21$ at 971 GHz. This model predicts that the column densities are similar to those at the background radiation temperature of 2.73 K under the same conditions of T_{kin} and $n(\text{H}_2)$ and the ortho-to-para ratio of water is $\sim 0.1 - 0.5$ (Table B.1).

4.2. Orion S

To estimate the column density for the absorption component of p-H₂¹⁸O 1₁₁ – 0₀₀, which is detected in Orion S, we derived the

optical depth using the expression

$$\tau = -\ln\left(\frac{T_{\text{line}}}{T_{\text{cont}}}\right) \quad (1)$$

where T_{cont} is the single side band (SSB) continuum intensity assuming that the continuum is completely covered by the absorbing layer and T_{line} is the intensity at the absorption dip with continuum. We apply a linear baseline fit in the vicinity of the absorption line to derive the continuum intensity (~ 4.6 K with uniform beam filling) at the absorption peak. Deriving the optical depth from the line-to-continuum ratio is based on the assumption that the excitation temperature is negligible with respect to the continuum temperature (i.e., no emission filling in the absorption) and that the line is not saturated.

If all water molecules are in the para ground-state, the velocity integrated absorption is related to the molecular column density by

$$N = \frac{8\pi\nu^3 g_l}{c^3 A g_u} \int \tau dV, \quad (2)$$

where N is the column density, ν the frequency, c the speed of light, and τ is the optical depth. A stands for the Einstein-A coefficient and g_l and g_u are the degeneracy of the lower and the upper level of the transition. Integrating between $V = 0$ and 13 km s⁻¹, we find a column density of $\sim 2.0 \times 10^{12}$ cm⁻² for the para-H₂¹⁸O line in Orion S.

Assuming LTE and using the same assumptions as for the Bar given the limit on the optical depth (< 0.7) by the non-detection of H₂¹⁷O and the T_{ex} limit (< 100 K) from the excited states, we find a beam-averaged column density of $\sim 2.0 \times 10^{11}$ cm⁻² for the ortho-H₂¹⁸O line. Thus, assuming LTE, the ortho-to-para ratio of water is ~ 0.1 in Orion S.

As before we perform a series of non-LTE calculations to confirm the low OPR derived for Orion S assuming LTE. We therefore generate a grid of models with values of T_{kin} and $n(\text{H}_2)$, and a background radiation field of 2.73 K. We find an OPR ~ 0.3 assuming $T_{\text{kin}} = 100$ K and $n(\text{H}_2) = 10^8$ cm⁻³, but derive a value of 3 (or unphysically higher than 3) if $T_{\text{kin}} = 60$ K and $n(\text{H}_2) = 10^6$ cm⁻³ or for $T_{\text{kin}} = 20$ K and $n(\text{H}_2) = 10^4$ cm⁻³. Thus the derived ortho-to-para ratio of water is strongly sensitive to the assumed physical conditions (Table B.1).

Further constraints on the OPR in Orion S come from the non-detection of the ortho-H₂¹⁸O 2₁₂ – 1₀₁ line (1655.9 GHz) in our survey. This line connects to the ortho-H₂O ground state and arises at a much higher frequency where the continuum level is higher (~ 6.1 K) than at the frequency of the para-H₂O ground state line. This non-detection of the ortho-H₂¹⁸O 2₁₂ – 1₀₁ line in either emission or absorption gives information on the limit of the ortho-H₂O column density in the absorbing gas. Assuming that the ground-state line of ortho-H₂¹⁸O 2₁₂ – 1₀₁ appears in absorption, we estimate its optical depth. We adopt a line width

of 5.5 km s^{-1} from the para- H_2^{18}O $1_{11} - 0_{00}$ line observations, a continuum intensity of 6.1 K, and a rms of 0.4 K from the ortho- H_2^{18}O $2_{12} - 1_{01}$ line observations. Assuming that the ortho-to-para ratios of water are 3, 2.5, 2, and 1, we derive a T_{line} of 4.8, 5.0, 5.2, and 5.6 K, respectively, using Eq. (1) and (2). If the ortho-to-para ratios of water are 3 and 2.5, we should see absorption lines of ortho- H_2^{18}O $2_{12} - 1_{01}$ with optical depth of 0.24 and 0.20, respectively. However, for ortho-to-para ratios of 1 and 2, the ortho- H_2^{18}O $2_{12} - 1_{01}$ would be seen in absorption with optical depth of 0.16 and 0.08 (within the noise), as illustrated in Fig. C.1. We conclude that our data are consistent with $\text{OPR} \leq 2$ for cold water, but not with $\text{OPR} \geq 2.5$.

5. Discussion

Our derived OPR of H_2O in the Orion Bar is $0.1 - 0.5$ ($T_{\text{spin}} \sim 8 - 12 \text{ K}$), which is well below that of other ISM sources and even lower than that toward TW Hya. It is also much lower than expected based on the gas temperature of $\sim 85 \text{ K}$ (Hogerheijde et al. 1995). Furthermore, the ortho-to-para ratio of water in Orion S is below 2 ($T_{\text{spin}} < 23 \text{ K}$).

Currently it is uncertain how low ortho-to-para ratios originate. Gas phase formation via H_3O^+ dissociative recombination is expected to lead to an OPR of 3 due the fact that the reaction is exothermic and the energy released is well in excess of the ortho/para energy difference (Hogerheijde et al. 2011). It cannot originate from grain surfaces due to thermal evaporation as the measured dust temperature towards the Bar (and presumably Orion S) is $\sim 35 - 70 \text{ K}$ (Arab et al. 2012) which is below the evaporation temperature of water ice ($\sim 100 \text{ K}$; Fraser et al. 2001).

The low water OPR may be explained by photodesorption, which has been argued to be the main formation mechanism for cold water vapor in the dense ISM (Hollenbach et al. 2009). In addition, a direct observational proof for photodesorption of H_2O is provided by the detection of gas-phase H_2O towards the pre-stellar core L1544 (Caselli et al. 2012) and NGC 1333-IRAS4A protostar (Mottram et al. 2013). There are two possible processes for photodesorption, following photodissociation of H_2O ice into H and OH after absorption of a UV photon (Andersson & van Dishoeck 2008; Arasa et al. 2010; Tielens 2013; van Dishoeck et al. 2013): 1) H and OH recombine in the ice to form H_2O , which then has sufficient energy to desorb, 2) the energetic H atom kicks out a neighboring H_2O molecule from the ice, which is initiated by the same UV photon. In option 1, the OPR should go to the statistical value of 3 because of the exothermicity of the reaction. In option 2, the original OPR in the ice should be preserved. So if the grain temperature is low and the OPR equilibrated to the grain temperature, the OPR should be low, in agreement with our results. The relative importance of option 1 and 2 depends on the thickness of the ice layer and to a lesser extent on the ice temperature. Roughly, they contribute about equally, but a detailed calculation is beyond the scope of this work. The experiments by Yabushita et al. (2009) show that the measured translational and rotational energies of H_2O ($v = 0$) molecules photodesorbed from amorphous solid water are in good agreement with those predicted by classical molecular dynamics calculations for the “kick-out” mechanism (option 2).

The ortho-to-para ratios of water have been measured in many different environments but the *Herschel*/HIFI H_2O observations in the Orion PDR show an unusually low ortho-to-para ratio of water. This opportunity will be further explored in a future paper, where we will estimate ortho-to-para ratio of other molecules in the Orion PDR, and we will compare ortho-to-para

ratio of water in other PDRs. In addition, the *Herschel*/HIFI H_2O observations toward the Orion PDR show the structure in more detail than any previous study. It will also be further study in a future paper, where we will estimate H_2O abundance profiles.

Acknowledgements. We thank the referee for the constructive suggestions. We also thank the editor Malcolm Walmsley for additional helpful comments. The authors thank Ewine van Dishoeck, Edith Fayolle, Jean-Hugh Fillion, and An-nemieke Petrigani for useful discussions on photodesorption. HIFI has been designed and built by a consortium of institutes and university departments from across Europe, Canada and the US under the leadership of SRON Netherlands Institute for Space Research, Groningen, The Netherlands with major contributions from Germany, France and the US. Consortium members are: Canada: CSA, UWaterloo; France: CESR, LAB, LERMA, IRAM; Germany: COSMA, MPfR, MPS; Ireland, NUI Maynooth; Italy: ASI, IFSI-INAF, Arcetri-INAF; Netherlands: SRON, TUD; Poland: CAMK, CBK; Spain: Observatorio Astronómico Nacional (IGN), Centro de Astrobiología (CSIC-INTA); Sweden: Chalmers University of Technology – MC2, RSS & GARD, Onsala Space Observatory, Swedish National Space Board, Stockholm University – Stockholm Observatory; Switzerland: ETH Zürich, FHNW; USA: Caltech, JPL, NHSC.

References

- Andersson, S. & van Dishoeck, E. F. 2008, *A&A*, 491, 907
 Arab, H., Abergel, A., Habart, E., et al. 2012, *A&A*, 541, A19
 Arasa, C., Andersson, S., Cuppen, H. M., van Dishoeck, E. F., & Kroes, G.-J. 2010, *J. Chem. Phys.*, 132, 184510
 Bergin, E. A., Phillips, T. G., Comito, C., et al. 2010, *A&A*, 521, L20
 Caselli, P., Keto, E., Bergin, E. A., et al. 2012, *ApJ*, 759, L37
 Cernicharo, J., Goicoechea, J. R., Pardo, J. R., & Asensio-Ramos, A. 2006, *ApJ*, 642, 940
 Daniel, F., Dubernet, M.-L., & Grosjean, A. 2011, *A&A*, 536, A76
 de Graauw, T., Helmich, F. P., Phillips, T. G., et al. 2010, *A&A*, 518, L6
 Draine, B. T. 1978, *ApJS*, 36, 595
 Flagey, N., Goldsmith, P. F., Lis, D. C., et al. 2013, *ApJ*, 762, 11
 Fraser, H. J., Collings, M. P., McCoustra, M. R. S., & Williams, D. A. 2001, *MNRAS*, 327, 1165
 Herrmann, F., Madden, S. C., Nikola, T., et al. 1997, *ApJ*, 481, 343
 Hogerheijde, M. R., Bergin, E. A., Brinch, C., et al. 2011, *Science*, 334, 338
 Hogerheijde, M. R., Jansen, D. J., & van Dishoeck, E. F. 1995, *A&A*, 294, 792
 Hollenbach, D., Kaufman, M. J., Bergin, E. A., & Melnick, G. J. 2009, *ApJ*, 690, 1497
 Hollenbach, D. J. & Tielens, A. G. G. M. 1999, *Reviews of Modern Physics*, 71, 173
 Larsson, B., Liseau, R., Bergman, P., et al. 2003, *A&A*, 402, L69
 Leurini, S., Rolfs, R., Thorwirth, S., et al. 2006, *A&A*, 454, L47
 Lis, D. C., Bergin, E. A., Schilke, P., & van Dishoeck, E. F. 2013, *Journal of Physical Chemistry A*, 117, 9661
 Lis, D. C. & Schilke, P. 2003, *ApJ*, 597, L145
 McMullin, J. P., Mundy, L. G., & Blake, G. A. 1993, *ApJ*, 405, 599
 Melnick, G. J., Tolls, V., Snell, R. L., et al. 2011, *ApJ*, 727, 13
 Menten, K. M., Reid, M. J., Forbrich, J., & Brunthaler, A. 2007, *A&A*, 474, 515
 Mezger, P. G., Zylka, R., & Wink, J. E. 1990, *A&A*, 228, 95
 Mottram, J. C., van Dishoeck, E. F., Schmalzl, M., et al. 2013, *A&A*, 558, A126
 Mumma, M. J. & Charnley, S. B. 2011, *ARA&A*, 49, 471
 Mumma, M. J., Weaver, H. A., & Larson, H. P. 1987, *A&A*, 187, 419
 Nagy, Z., Van der Tak, F. F. S., Ossenkopf, V., et al. 2013, *A&A*, 550, A96
 Ossenkopf, V., Röllig, M., Cubick, M., & Stutzki, J. 2007, in *Molecules in Space and Laboratory*
 Ott, S. 2010, in *Astronomical Society of the Pacific Conference Series*, Vol. 434, *Astronomical Data Analysis Software and Systems XIX*, ed. Y. Mizumoto, K.-I. Morita, & M. Ohishi, 139
 Peng, T.-C., Wyrowski, F., Zapata, L. A., Güsten, R., & Menten, K. M. 2012, *A&A*, 538, A12
 Pilbratt, G. L., Riedinger, J. R., Passvogel, T., et al. 2010, *A&A*, 518, L1
 Roelfsema, P. R., Helmich, F. P., Teyssier, D., et al. 2012, *A&A*, 537, A17
 Schöier, F. L., van der Tak, F. F. S., van Dishoeck, E. F., & Black, J. H. 2005, *A&A*, 432, 369
 Simon, R., Stutzki, J., Sternberg, A., & Winnewisser, G. 1997, *A&A*, 327, L9
 Tielens, A. G. G. M. 2013, *Reviews of Modern Physics*, 85, 1021
 Ungerechts, H., Bergin, E. A., Goldsmith, P. F., et al. 1997, *ApJ*, 482, 245
 van der Tak, F. F. S., Black, J. H., Schöier, F. L., Jansen, D. J., & van Dishoeck, E. F. 2007, *A&A*, 468, 627
 van Dishoeck, E. F., Herbst, E., & Neufeld, D. A. 2013, *Chemical Reviews*, 113, 9043
 Yabushita, A., Hama, T., Yokoyama, M., et al. 2009, *ApJ*, 699, L80
 Young Owl, R. C., Meixner, M. M., Wolfire, M., Tielens, A. G. G. M., & Tauber, J. 2000, *ApJ*, 540, 886
 Zapata, L. A., Ho, P. T. P., Rodríguez, L. F., et al. 2006, *ApJ*, 653, 398

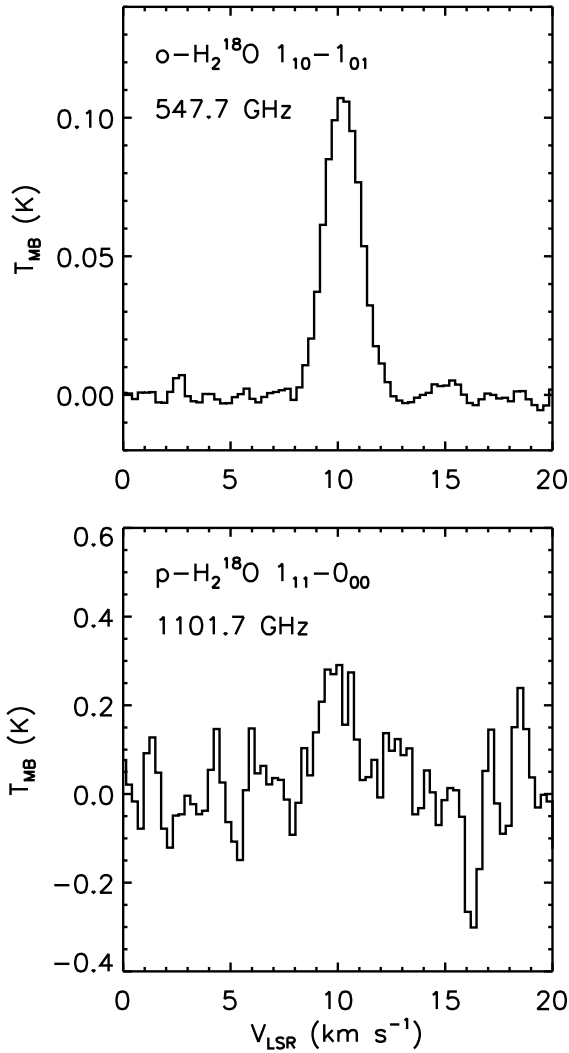


Fig. A.1. Spectra of the ground-state H_2^{18}O lines in the Orion Bar. The weak continuum has been subtracted.

Appendix A: Spectra of the ground-state H_2^{18}O lines

In Sect. 3, we present the ground-state lines of ortho- and para- H_2^{18}O observed with *Herschel*/HIFI toward the Orion Bar (Fig. A.1) and Orion S (Fig. A.2).

Appendix B: Column densities derived by non-LTE RADEX code

In Sect. 4, for the non-LTE calculations of ortho- and para- H_2^{18}O lines we generate a grid of models with values of $T_{\text{kin}} = 20, 60,$ and 100 K, values of $n(\text{H}_2) = 10^4, 10^6,$ and 10^8 cm^{-3} , and fix the background radiation temperature at 2.73 K for the Orion Bar and Orion S using the RADEX code (van der Tak et al. 2007). Table B.1 presents the derived column densities for the adopted conditions from a full grid non-LTE calculations as examples. The p- H_2^{18}O $1_{11}-0_{00}$ line in Orion S appears in absorption so we derive the column density using the optical depth (see Sect. 4.2 for details).

As an additional model for the Orion Bar, for the background radiation field we adopt a modified blackbody distribution with

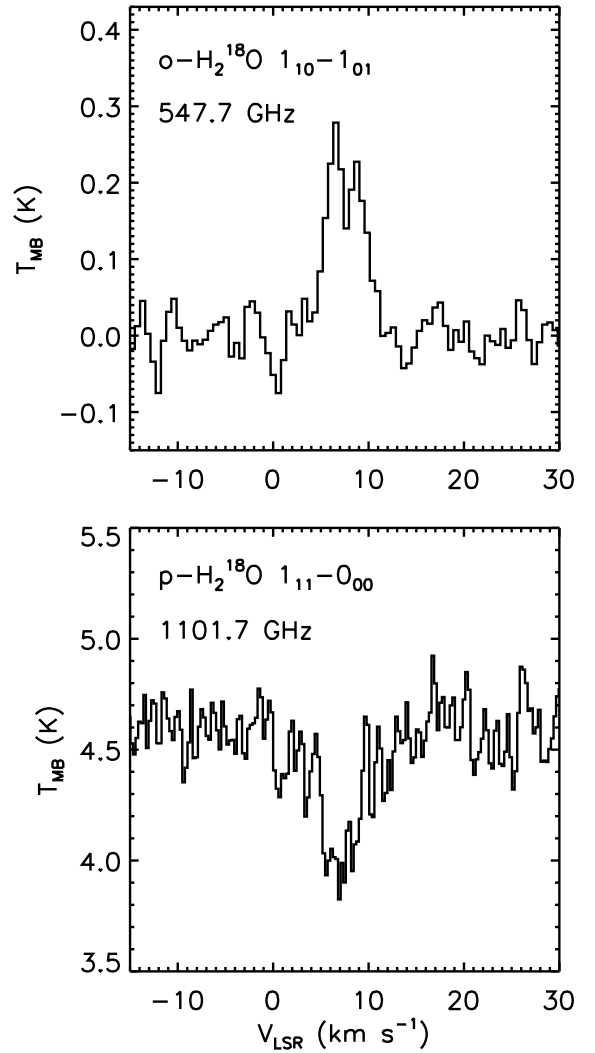


Fig. A.2. Spectra of the ground-state H_2^{18}O lines toward Orion S. For the o- H_2^{18}O line, the continuum has been subtracted. The p- H_2^{18}O line shows absorption against the continuum.

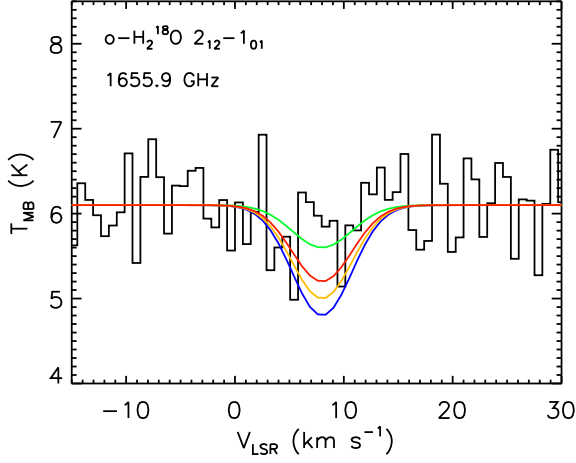
a dust temperature of $T_d = 49$ K and a dust emissivity index of $\beta = 1.6$ by Arab et al. (2012) for the interior of the Orion Bar, so that the absolute dust opacity of $\tau_d = 0.21$ at 971 GHz. This RADEX model shows that ortho- and para- H_2^{18}O lines appear in absorption at the low density and low temperature (at $T_{\text{kin}} = 20$ K & $n(\text{H}_2) = 10^4$ cm^{-3}), which is not consistent with our observations.

Appendix C: Further constraints on the OPR in Orion S

In Sect. 4.2, we estimate the intensity of the ground-state line of ortho- H_2^{18}O $2_{12}-1_{01}$ (1655.9 GHz) assuming that this line appears in absorption to constrain the OPR in Orion S. In Fig. C.1 we present four absorption lines on top of the ground-state ortho- H_2^{18}O $2_{12}-1_{01}$ line. The green, red, yellow, and blue lines represent absorption lines with optical depth of $0.08, 0.16, 0.20,$ and $0.24,$ respectively.

Table B.1. Examples of column densities for the adopted conditions from a full grid non-LTE calculations in the Orion Bar and Orion S.

Source	Molecule	Transition	T_{kin} & $n(\text{H}_2)$ (K & cm^{-3})		
			20 & 10^4	60 & 10^6	100 & 10^8
N from RADEX Model with $T_{\text{bg}} = 2.73$ K (cm^{-2})					
Orion Bar	o- H_2^{18}O	$1_{10} - 1_{01}$	2.19×10^{15}	1.65×10^{12}	1.20×10^{11}
	p- H_2^{18}O	$1_{11} - 0_{00}$	3.08×10^{16}	1.75×10^{13}	2.66×10^{11}
Orion S	o- H_2^{18}O	$1_{10} - 1_{01}$	1.13×10^{16}	8.57×10^{12}	6.06×10^{11}
N from RADEX Model with $T_{\text{d}} = 49$ K & $\beta = 1.6$ (cm^{-2})					
Orion Bar	o- H_2^{18}O	$1_{10} - 1_{01}$	–	2.80×10^{12}	1.49×10^{11}
	p- H_2^{18}O	$1_{11} - 0_{00}$	–	2.01×10^{13}	2.96×10^{11}


Fig. C.1. Four absorption lines on top of spectra of the ground-state ortho- H_2^{18}O $2_{12}-1_{01}$ line (black), with continuum in Orion S. Assuming that the OPRs are 1, 2, 2.5, and 3, the derived optical depth of 0.08, 0.16, 0.20, and 0.24 are presented, respectively, as green, red, yellow, and blue.